



# Primary histiocytic sarcoma in the brain with renal metastasis causing internal ophthalmoparesis and external ophthalmoplegia in a Maine Coon cat

*Journal of Feline Medicine and Surgery Open Reports*  
1–7

© The Author(s) 2021

Article reuse guidelines:

sagepub.com/journals-permissions

DOI: 10.1177/20551169211038515

journals.sagepub.com/home/jfmsopenreports

This paper was handled and processed by the European Editorial Office (ISFM) for publication in *JFMS Open Reports*



Susana Monteiro, Katherine Hughes<sup>id</sup>, Marie-Aude Genain and Lisa Alves

## Abstract

**Case summary** An 11-year-old neutered male Maine Coon cat was presented for investigation of anisocoria and depression. Neurological examination was consistent with a lesion at the level of the middle cranial fossa, and biochemistry was indicative of moderate renal functional impairment. MRI of the brain identified an extra-axial mass lesion at the level of the middle cranial fossa, T2-weighted hyperintense and strongly homogeneously contrast enhancing with dural tail. The cat was euthanased after 6 weeks of palliative treatment with corticosteroids. Histopathology and immunohistochemistry of the brain, the intra-cranial mass and the renal masses found on necropsy were consistent with histiocytic sarcoma.

**Relevance and novel information** Central nervous system histiocytic sarcoma is a rare finding in cats. This original case report describes the neurological presentation, novel MRI characteristics and pathological findings of suspected primary histiocytic sarcoma affecting the brain with renal metastasis in a cat.

**Keywords:** Neoplasia; intracranial; cat; middle cranial fossa; dural tail

**Accepted:** 22 July 2021

## Case description

An 11-year-old castrated male Maine Coon cat was presented with a 3-week history of depressed mental status and anisocoria, with the right pupil larger than the left pupil. The cat also had suspected lumbar and abdominal discomfort, and had been placed on meloxicam (0.1 mg/kg q24h PO) and gabapentin (4 mg/kg q12h PO) ongoing 1 week prior to presentation.

General physical examination was unremarkable, including palpation of both kidneys. On neurological examination the cat was depressed but responsive and interacted normally with its environment. Menace response and dazzle reflex were present and normal bilaterally. Marked anisocoria was present, with mydriasis in the right eye. Direct and consensual pupillary light reflexes were severely reduced in the right eye but

normal in the left eye. The right eye also demonstrated ptosis, protrusion of the third eyelid and an absence of both spontaneous physiological nystagmus and vestibulo-ocular reflex. Based on the neurological examination findings, a disease process affecting the right oculomotor nerve (both parasympathetic and motor components) and right sympathetic innervation of the eye was suspected, likely at its pathway through the middle cranial fossa or at the level of the mesencephalon.

Department of Veterinary Medicine, University of Cambridge, Cambridge, UK

### Corresponding author:

Susana Monteiro DVM, Department of Veterinary Medicine, University of Cambridge, Madingley Road, Cambridge CB3 0ES, UK  
Email: sm926@cam.ac.uk



Creative Commons Non Commercial CC BY-NC: This article is distributed under the terms of the Creative Commons

Attribution-NonCommercial 4.0 License (<https://creativecommons.org/licenses/by-nc/4.0/>) which permits non-commercial use, reproduction and distribution of the work without further permission provided the original work is attributed as specified on the SAGE and Open Access pages (<https://us.sagepub.com/en-us/nam/open-access-at-sage>).

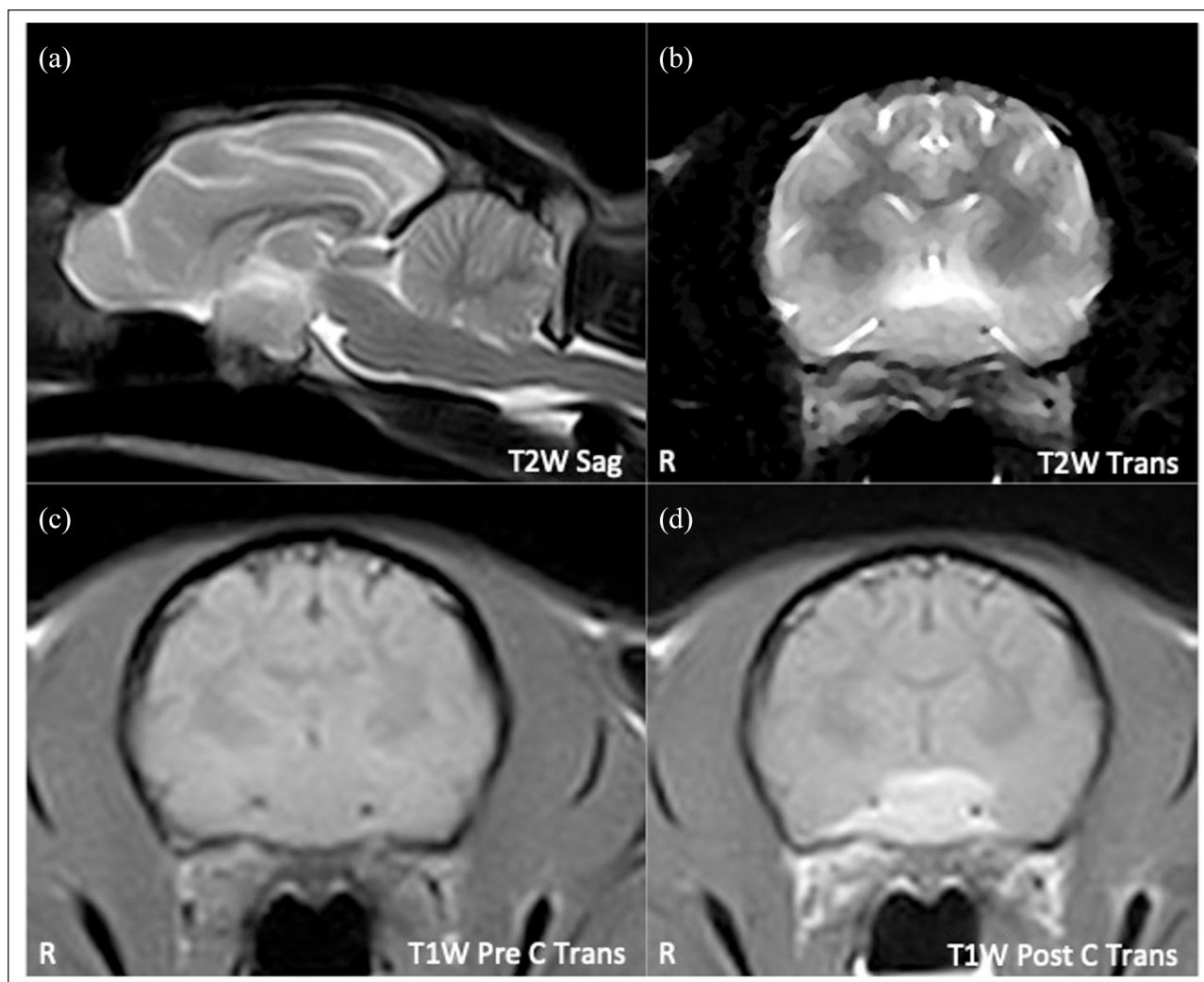


**Figure 1** Composite of the MRI images of the Maine Coon cat's brain, showing a large T2-weighted hyperintense to the cerebral grey matter extra-axial lesion at the level of the pituitary and middle cranial fossa (a: sagittal view; b: transverse view). The lesion is T1-weighted mildly hypointense to the cerebral grey matter (c) and shows strong, homogeneous contrast enhancement, including the presence of dural tails (d)

Haematology results were unremarkable. Complete serum biochemistry revealed mild hypernatraemia (160 mmol/l; reference interval [RI] 135–155), an increase in urea (11.6 mmol/l; RI 5.4–6.7) and creatinine (267  $\mu$ mol/L; RI 56–153), and a mild increase in total protein (81 g/l; RI 56–78) and globulin (48 g/l; RI 24–47). Urinalysis revealed a specific gravity of 1.018 but no other abnormalities. Serology for *Toxoplasma gondii* showed an increase in IgG concentration (positive at 1:400) and normal IgM, compatible with previous exposure to the pathogen. Cisternal cerebrospinal fluid (CSF) analysis revealed hyperproteinuria, with a microprotein value of 0.58 g/l and normal cell count and morphology.

MRI of the brain using a 0.27 T magnet (MRI Grande; Esaote) was performed and the following sequences acquired: sagittal, transverse and dorsal T2-weighted

(T2W), sagittal, transverse and dorsal T1-weighted (T1W), transverse gradient echo T2, transverse fluid-attenuated inversion recovery (FLAIR), and transverse three-dimensional hybrid contrast enhancement (HYCE). Following intravenous administration of a gadolinium-based contrast medium (Gadovist; Bayer) at a dose of 0.1 mmol/kg, all three T1W sequences were repeated.

At the level of the middle cranial fossa and pituitary fossa there was a partially well-defined, extra-axial mass lesion (Figure 1). The lesion involved the optic chiasm. This mass was T2W mildly hyperintense and T1W mildly hypointense to the cerebral grey matter and FLAIR isointense, except on its dorsal aspect, where it did not suppress and was strongly hyperintense. Moderate peri-tumoral oedema was evident. Strong, homogeneous contrast enhancement that included the

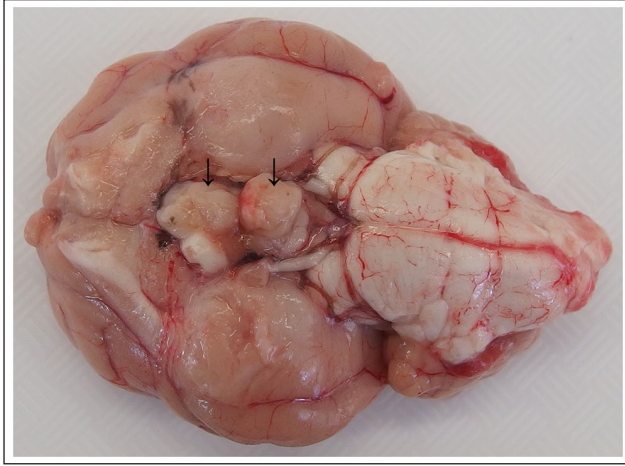


**Figure 2** Ventral aspect of the brain. The left optic nerve, and, to a lesser extent, oculomotor nerve, and the pituitary gland, are obscured by an unencapsulated, moderately poorly demarcated, homogeneous, moderately firm white mass (arrows)

presence of dural tails in all directions was seen, as well as enhancement of both the right optic and oculomotor nerves.

Given the clinical presentation, MRI findings and CSF results, a presumptive diagnosis of a neoplastic process was made, most likely a basal meningioma, lymphoma, craniopharyngioma or histiocytic sarcoma (HS).

Following the diagnostic tests, the cat was started on prednisolone (0.5 mg/kg q24h ad eternum), as further investigation (or treatment), including abdominal ultrasound, thoracic radiographs and urinary culture and sensitivity, to confirm the altered renal parameters and to find another neoplastic focus, were declined. At the 2-week recheck, the cat's mentation and behaviour were normal, and the right eye exhibited less pronounced mydriasis, reduced but present pupillary light reflex (both direct and consensual), and protrusion of the third eyelid. The external ophthalmoplegia had resolved. At the 6-week recheck, the cat had deteriorated and was presented as depressed and compulsively circling to the right. The right-sided cranial nerve deficits related to the sympathetic supply and oculomotor nerve were again present but less pronounced than the prior presentation. Euthanasia and post-mortem examination were performed.

The key findings noted at gross post-mortem examination were that the optic nerves, and, to a lesser extent, oculomotor nerves, and the pituitary gland, were obscured by an unencapsulated, moderately poorly demarcated, homogeneous, moderately firm white mass that was multinodular (Figure 2). From a main nodule, the mass indistinctly spread and infiltrated, in a thin layer, >80% of the ventral aspect of the cranial vault (Figure 3). The right and left kidneys exhibited a round 3–8 mm diameter, respectively, white, homogeneous,

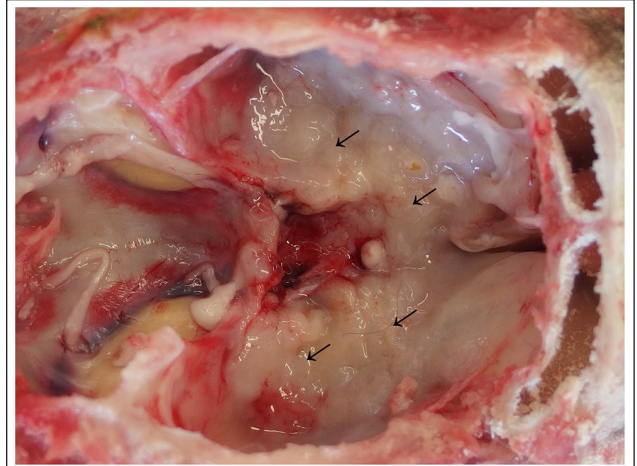


**Figure 3** Cranial vault. The neoplastic mass infiltrates widely across the ventral aspect of the cranial vault (arrows)

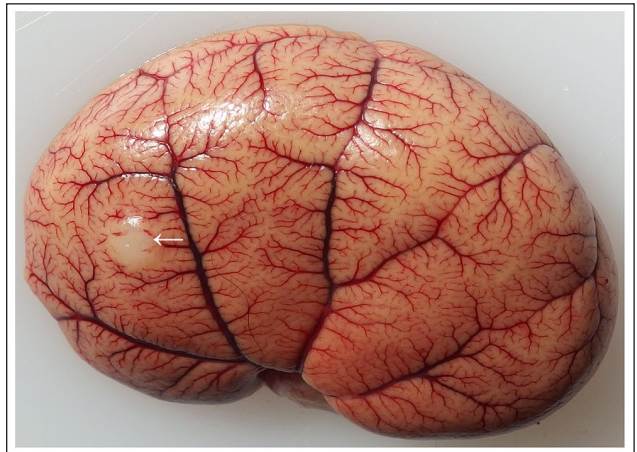


**Figure 4** Kidney. The parenchyma is expanded by a well-demarcated, unencapsulated, cream nodule (arrow)

unencapsulated but well-demarcated, moderately firm mass (Figure 4).

For histological evaluation, the brain and tissue samples from a panel of organs were fixed in 10% neutral buffered formalin solution. Following fixation, samples were processed, paraffin embedded and sectioned following routine histological protocols. Histological examination revealed that the optic chiasm, and ventral aspects of the hypothalamus and piriform lobes were compressed and infiltrated by a moderately densely cellular and unencapsulated neoplastic mass (Figure 5). The neoplastic cells, loosely arranged in sheets, were round to polygonal, with frequently clearly delineated cell boundaries. The nuclei were round to oval or reniform, and with a variable number of frequently prominent basophilic nucleoli. There were 15 mitoses in 10 high-power fields (per 2.37 mm<sup>2</sup>), and there was moderate anisocytosis, and marked anisokaryosis, and nuclear pleomorphism. Scattered

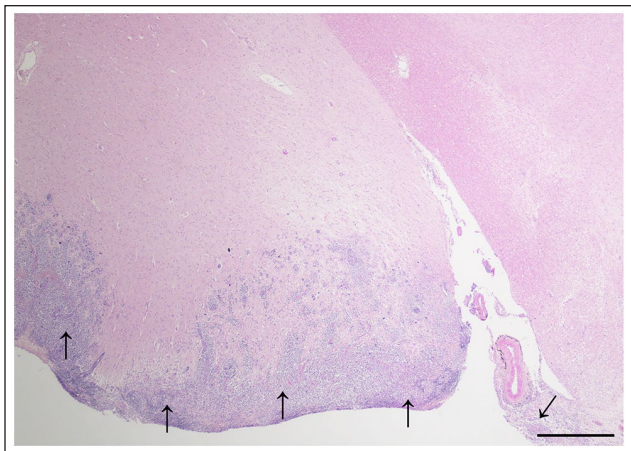


**Figure 5** Ventral aspect of the brain. The piriform lobes and hypothalamus are infiltrated by a moderately densely cellular and unencapsulated neoplastic mass (arrows). Haematoxylin and eosin stain. Scale bar = 800  $\mu$ m

multifocally were groupings of moderate-to-large numbers of lymphocytes with fewer plasma cells. Multifocally these formed prominent perivascular cuffs. Multifocally, perivascular cuffs included variable proportions of admixed neoplastic cells.

The renal parenchyma was expanded by a neoplastic population with similar histological features to that in the brain (Figure 6).

Immunohistochemical (IHC) staining for CD3 (dilution 1:150; mouse monoclonal, clone F7.2.38 [Dako Pathology/Agilent Technologies]), MHCII (dilution 1:400; HLA-DR antigen alpha chain, mouse monoclonal, clone TAL.1B5 [Dako Pathology/Agilent Technologies]) and Iba1 (dilution 1:800; mouse monoclonal, clone 20A12.1 [Millipore]), followed a routine protocol using

EnVision FLEX high pH target antigen retrieval solution (Dako Pathology/Agilent Technologies).

IHC staining revealed that the majority of the neoplastic cells in both the kidney (Figure 6) and the brain (Figure 7) exhibited intense cytoplasmic and membranous expression of Iba1. Additional IHC staining performed on the neoplastic population within the brain demonstrated that the majority of the neoplastic cells also exhibited intense cytoplasmic and membranous expression of MHCII, and were infiltrated by moderate-to-large numbers of lymphocytes exhibiting intense membranous staining for CD3 (Figure 7).

Taken together, it was considered that the gross, microscopic and IHC findings were consistent with a primary HS of the brain that had metastasised to the kidneys bilaterally.

## Discussion

Feline HS is a rare neoplastic process that can affect several locations,<sup>1-10</sup> including the central nervous system (CNS). To date, only four feline cases of CNS HS have been described.<sup>11-14</sup> Three presented with brain involvement as a single lesion,<sup>11</sup> part of unusual multifocal histiocytic disease<sup>12</sup> or unclassified.<sup>14</sup> The fourth case described a mediastinal mass with dura mater and spinal cord involvement.<sup>13</sup> Our report describes a new presentation of feline brain/pituitary fossa HS with MRI characteristics of an extra-axial mass with meningeal enhancement, similar to the ones most commonly found in canine patients.

When HS presents in more than one organ, the origin of the neoplastic process is often difficult to ascertain. Both multicentric disease and a primary tumour with metastatic spread are included under the nomenclature 'disseminated HS'.<sup>10,15</sup> In our case, a primary CNS focus

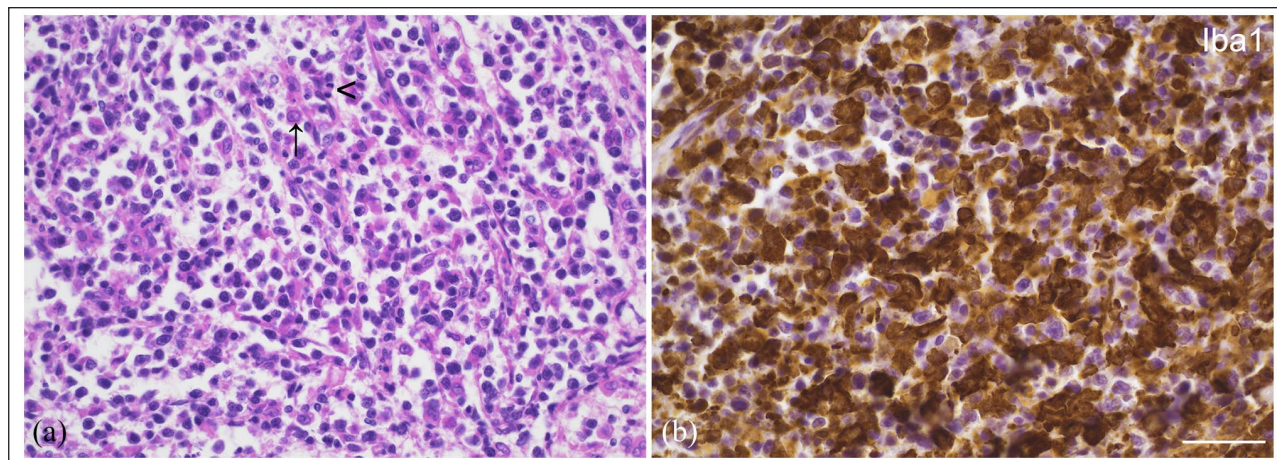


**Figure 6** Kidney. The renal parenchyma is infiltrated by a moderately densely cellular round-cell neoplasm. Note the mitotic figure (arrowhead) and the reniform appearance of some of the nuclei (arrow). The majority of the neoplastic cells exhibit intense cytoplasmic and membranous expression of Iba1. (a) Haematoxylin and eosin stain. (b) Immunohistochemistry staining for Iba1 with haematoxylin counterstain. Scale bar = 800  $\mu$ m

was suspected, with a much larger brain lesion as the potential original site. The bilateral distribution of the round renal masses was consistent with metastatic disease, as described in humans.<sup>16</sup> The presumed metastatic renal disease was only detected on necropsy, although International Renal Interest Society stage 3 chronic kidney disease was suspected ante-mortem, accounting for the laboratory findings.

CNS HS in humans is extremely rare,<sup>17,18</sup> and metastatic-associated disease even more so, with only one unpublished report of spontaneous metastatic spread.<sup>19</sup> Disseminated forms of HS with CNS involvement have been described in dogs,<sup>20,21</sup> with different associated sites, including the kidneys.<sup>21</sup>

HSs can be divided into haemophagocytic and non-haemophagocytic.<sup>10</sup> The latter, as suspected in our case, originates from interstitial dendritic cells, which are present in perivascular locations in several organs. Although the CNS parenchyma is often not a site for these cells

owing to its unique immunological characteristics,<sup>15</sup> they can be found not only in the meninges and choroid plexus, but also in the circumventricular organs (CVOs), which lack a blood–brain barrier (BBB), and glia limitans in healthy mammals.<sup>20,21</sup> Interestingly, in both this case and the two reports of cats with brain HS where neuro-anatomical localisation was provided, the neoplasia was found in association with either the meninges or the ventricular system/CVOs.<sup>11,12</sup> In this case, a meningeal or a perivascular origin was suspected, taking into account the extensive dural tail observed on the MRI. In dogs CNS HS is commonly rostromentorial,<sup>22,23</sup> and no location preference has been seen in humans with primary CNS HS.<sup>24</sup> Interstitial dendritic cells can also be encountered all across the CNS parenchyma when the BBB or glia limitans are compromised, commonly with neuroinflammation.<sup>20,21</sup> Inflammatory foci are often encountered in 60% of humans with CNS HS,<sup>18,25</sup> and infiltration of the neoplastic lesion by CD3<sup>+</sup> cells (lymphocytes) has

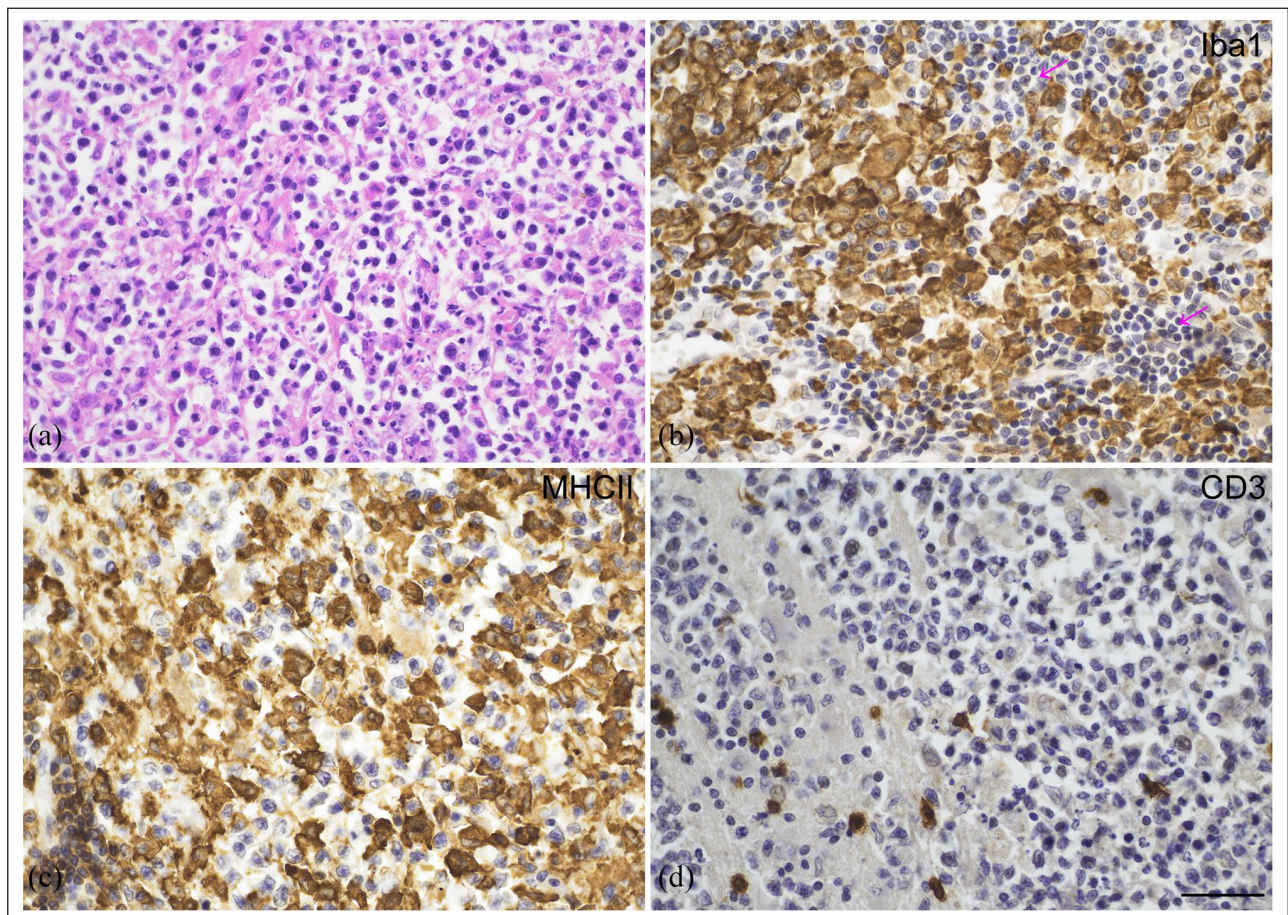


**Figure 7** Ventral aspect of the brain. The neoplastic cells exhibit morphology and immunohistochemical (IHC) staining properties consistent with a histiocytic sarcoma. Note the infiltration with lymphocytes that multifocally form dense groupings (magenta arrows). (a) Haematoxylin and eosin stain. (b) IHC staining for Iba1, (c) MHCII and (d) CD3 with haematoxylin counterstain. Scale bar = 40  $\mu$ m

also been found in feline HS<sup>11</sup> and in dogs,<sup>26</sup> as in this case. This leads to the question of whether a primary CNS inflammation could be, or contribute to, the origin of CNS HS, or if the inflammation is secondary to the neoplasia.<sup>27,28</sup>

In the few reports of HS with brain involvement,<sup>11,12</sup> older cats (8–13 years of age) similar to this patient seem to be affected. In humans or dogs there is no obvious age predisposition.<sup>18,20</sup> Clinical signs are related to the neuroanatomical localisation and involvement of other systems.<sup>5</sup> In this case, the CNS lesion distribution was mainly diffuse bilateral; however, the signs were consistent with a right-sided intracranial neuroanatomical localisation. The right-sided cranial nerve dysfunction became less apparent once the corticosteroid course was started, probably by addressing the peri-tumoral oedema. However, circling to the right had developed by the last presentation and disease progression was suspected.

The MRI description of the feline brain CNS previously reported was similar regarding intensities in T1W and T2W sequences, oedema and contrast enhancement.<sup>11</sup> However, in that case no dural tail was described. Our case shares the imaging characteristics commonly described in canine CNS HS such as extra-axial masses associated with peri-tumoral oedema, and variable T2W intensity, mixed FLAIR intensity that often presents a dural tail.<sup>23,29</sup>

Definitive diagnosis of HS requires morphological and immunological confirmation of the histiocytic lineage of the malignancy. We used Iba1 and MHCII as the primary antibody-positive markers for feline HS. Iba1 is a microglial/macrophage marker, and it is not expressed by lymphocytes.<sup>11</sup> MHCII (antigen-presenting cell marker) positivity is consistent with histiocytic disease, but its use had not been described in CNS feline HS, although it is used in this disease in feline patients.<sup>2,4,6</sup>

Different genetic mutations have been found in people presenting with CNS HS through genomic sequencing, including *PDGRF*,<sup>18</sup> *BRAF V600E*<sup>30</sup> and *PTPN11* mutations. Recently, in dogs with non-CNS HS, the *PTPN11* mutation has also been identified,<sup>31,32</sup> as has a mutation on *KRAS*.<sup>32</sup> Currently, in humans and dogs, treatment includes CNS surgery, together with radiotherapy and/or chemotherapy.<sup>17,18,22</sup> In dogs with disseminated CNS HS, often only one, if any, treatment modality is instituted.<sup>22</sup> There is only one report of chemotherapeutic management (initially prednisolone and cytosine arabinoside, then with the addition of doxorubicin) of a cat with suspected CNS lymphoma, later proven to be CNS HS.<sup>11</sup> Palliative treatment with corticosteroids was chosen for our patient with the goal of reduction of peri-tumoral oedema, as further staging and invasive procedures had been declined. Prognosis of cats with CNS HS is considered poor, although there are no data on response to treatment.

## Conclusions

This report described a case of a cat presenting with signs of intracranial dysfunction due to HS in the brain, and concomitant renal spread. A primary CNS site was suspected, with the renal lesions likely being a result of metastatic disease. HS should be included as a differential diagnosis for intracranial neoplasia in cats, particularly if presenting meningeal involvement.

**Acknowledgements** The authors thank Debbie Sabin for her expertise in preparing the histological sections and performing the immunohistochemical staining.

**Conflict of interest** The authors declared no potential conflicts of interest with respect to the research, authorship, and/or publication of this article.

**Funding** The authors received no financial support for the research, authorship, and/or publication of this article.

**Ethical approval** The work described in this manuscript involved the use of non-experimental (owned or unowned) animals. Established internationally recognised high standards ('best practice') of veterinary clinical care for the individual patient were always followed and/or this work involved the use of cadavers. Ethical approval from a committee was therefore not specifically required for publication in *JFMS Open Reports*. Although not required, where ethical approval was still obtained, it is stated in the manuscript

**Informed consent** Informed consent (verbal or written) was obtained from the owner or legal custodian of all animal(s) described in this work (experimental or non-experimental animals, including cadavers) for all procedure(s) undertaken (prospective or retrospective studies). No animals or people are identifiable within this publication, and therefore additional informed consent for publication was not required.

**ORCID ID** Katherine Hughes  <https://orcid.org/0000-0002-3331-1249>

## References

- Hirabayashi M, Chambers JK, Sumi A, et al. **Immunophenotyping on nonneoplastic and neoplastic histiocytes in cats and characterization of a novel cell line derived from feline progressive histiocytosis.** *Vet Pathol* 2020; 57: 758–773.
- Teshima T, Hata T, Nezu Y, et al. **Amputation for histiocytic sarcoma in a cat.** *J Feline Med Surg* 2006; 14: 147–150.
- Pinard J, Wagg CR, Girard C, et al. **Histiocytic sarcoma in the tarsus of a cat.** *Vet Pathol* 2006; 43: 1014–1017.
- Bisson J, Van der Steen N, Hawkins I, et al. **Mediastinal histiocytic sarcoma with abdominal metastasis in a Somali cat.** *Vet Rec Case Rep* 2017; 5 e000405.
- Santifort K, Jurgens B, Grinwis GCM, et al. **Invasive nasal histiocytic sarcoma as the cause of temporal lobe epilepsy in a cat.** *JFMS Open Rep* 2018; 4. DOI: 10.1177/2055116918811179.

- 6 Scurrel E, Trott A, Rozmanee M, et al. **Ocular histiocytic sarcoma in a cat.** *Vet Ophthalmol* 2013; 16: 173–176.
- 7 Wong VM, Snyman HN, Ackerley C, et al. **Primary nasal histiocytic sarcoma of macrophage-myeloid cell type in a cat.** *J Comp Path* 2012; 147: 209–213.
- 8 Miyamoto R, Kurita S, Tani H, et al. **Establishment and characterization of a cell line from a feline histiocytic sarcoma.** *Vet Immunol Immunopathol* 2018; 201: 72–76.
- 9 Necova S, North S, Cahalan S, et al. **Oral histiocytic sarcoma in a cat.** *JFMS Open Rep* 2020; 6. DOI: 10.1177/2055116920971248.
- 10 Moore PF. **A review of histiocytic diseases of dogs and cats.** *Vet Pathol* 2014; 51: 167–184.
- 11 Ide T, Kazuyuki U, Tamura S, et al. **Histiocytic sarcoma in the brain of a cat.** *J Vet Med Sci* 2010; 72: 99–102.
- 12 Reed N, Begara-McGorum IM, Else RW, et al. **Unusual histiocytic disease in a Somali cat.** *J Feline Med Surg* 2005; 8: 129–134.
- 13 Smoliga J, Schatzerberg S, Peters J, et al. **Myelopathy caused by a histiocytic sarcoma in a cat.** *J Small Anim Pract* 2005; 46: 34–38.
- 14 Vernau KM, Higgins RJ, Bollen AW, et al. **Primary canine and feline nervous system tumors: intraoperative diagnosis using the smear technique.** *Vet Pathol* 2001; 38: 47–57.
- 15 Williams LE. **Canine and feline histiocytic diseases.** In: Ettinger SJ, Feldman EC and Cote E (eds). *Textbook of veterinary internal medicine*. 8th ed. St Louis, MO: Elsevier, 2017, pp 2115–2119.
- 16 Roy A, Le O, Silverman PM, et al. **Common and uncommon bilateral adult renal metastasis.** *Cancer Imaging* 2012; 12: 205–211.
- 17 Schuang M, Schild M, Tran D, et al. **Primary central nervous system histiocytic sarcoma. A case report and review of literature.** *Medicine* 2018; 97: 26. DOI: 10.1097/MD.00000000000011271.
- 18 May JM, Waddle MR, Miller DH, et al. **Primary histiocytic sarcoma of the central nervous system: a case report with platelet derived growth factor receptor mutation and PD-L1/PD-L2 expression and literature review.** *Radiat Oncol* 2018; 13: 167. DOI: 10.1186/s13014-018-1115-x.
- 19 Oštrić D, Todosijević M, Jeričević A, et al. **Brain pathology case of the month – August 2016.** Department of Pathology, University of Pittsburgh, 2016 (unpublished).
- 20 Mastorakos P and McGavern D. **The anatomy and immunology of vasculature in the central nervous system.** *Sci Immunol* 2019; 4: eaav0492. DOI: 10.1126/sciimmunol.aav0492.
- 21 D’Agostino PM, Gottfried-Blackmore A, Anandasbapathy N, et al. **Brain dendritic cells: biology and pathology.** *Acta Neuropathol* 2012; 124: 599–614.
- 22 Toyoda I, Vernau W, Sturges BK, et al. **Clinicopathological characteristics of histiocytic sarcoma affecting the central nervous system in dogs.** *J Vet Intern Med* 2020; 34: 828–837.
- 23 Mariani CL, Jennings MK, Olby NJ, et al. **Histiocytic sarcoma with central nervous system involvement in dogs: 19 cases (2006–2012).** *J Vet Intern Med* 2015; 29: 607–613.
- 24 So H, Kim SA, Yoon DH, et al. **Primary histiocytic sarcoma of the central nervous system.** *Cancer Res Treat* 2015; 47: 322–328.
- 25 Zanelli M, Ragazzi M, Marchetti G, et al. **Primary histiocytic sarcoma presenting as diffuse leptomeningeal disease: case description and review of the literature.** *Neuropathology* 2017; 37: 517–525.
- 26 Suzuki M, Uchida K, Morozumi M, et al. **A comparative pathological study on granulomatous meningoencephalomyelitis and central malignant histiocytosis in dogs.** *J Vet Med Sci* 2003; 65: 1319–1324.
- 27 Ruple-Czerniak A and Morley PS. **Evidence chronic inflammation is a risk factor for histiocytic sarcoma in Bernese mountain dogs – implications for human histiocytic sarcoma.** Proceedings of the 107th Annual Meeting of the American Association for Cancer Research; 2016 Apr 16–20; New Orleans, LA, USA. Philadelphia, PA: AACR; *Cancer Res* 2016; 76 14 Suppl: 3429.
- 28 Radons J. **Inflammatory stress and sarcomagenesis: a vicious interplay.** *Cell Stress Chaperones* 2014; 19: 1–13. DOI: 10.1007/s12192-013-0449-4.
- 29 Tamura S, Tamura Y, Nakamoto Y, et al. **MR imaging of histiocytic sarcoma of the canine brain.** *Vet Radiol Ultrasound* 2009; 50: 178–181.
- 30 Idbaih A, Mokhtari K, Emile JF, et al. **Dramatic response of a BRAF V600E mutated primary CNS histiocytic sarcoma to vemurafenib.** *Neurology* 2014; 83: 1478–1480.
- 31 Hedan B, Rault M, Abadie J, et al. **PTPN11 mutations in canine and human disseminated histiocytic sarcoma.** *Int J Cancer* 2020; 147: 1657–1665.
- 32 Takada M, Smyth LA, Thaiwong T, et al. **Activating mutations in PTPN11 and KRAS in canine histiocytic sarcoma.** *Genes (Basel)* 2019; 10: 505. DOI: 10.3390/genes10070505.